2024 IEEE/RSJ International Conference on Intelligent Robots and Systems (IROS)
October 14-18, 2024. Abu Dhabi, UAE

Robust Backstepping Controller with Adaptive Sliding Mode Observer for a Tilt-Augmented Quadrotor With Uncertainty Using $SO(3)$

Sathyanarayanan Seshasayanan, and Soumya Ranjan Sahoo

***Abstract*— The conventional quadrotor is incapable of controlling position and orientation independently. To mitigate this deficiency, we use a tilt-augmented quadrotor for greater mobility in a constrained environment. When the rotors tilt in a tilt-augmented quadrotor, it leads to changes in moment-of-inertia. This changes in the moment-of-inertia and external disturbances will introduce uncertainty terms into the model. In this paper, we design an adaptive super twisting sliding mode observer which guarantees finite time estimation of uncertain terms with unknown maximum bound. With the help of this observer, a backstepping controller using $SO(3)$ is developed to establish exponential convergence to the desired trajectory. The exponential convergence of the backstepping controller and finite time convergence of the observer are shown using the Lyapunov approach. Hardware experiments are performed to compare the performance of both the existing controller and our proposed controller and corresponding videos are at https://www.youtube.com/watch?v=brTd5UYvciM.**

I. INTRODUCTION

In the recent decades, quadrotors have gained recognition in both industrial and military sectors, for example, aerial photography, surveillance, and search and rescue missions. This is due to their compact size, vertical take-off and landing capabilities, agility, and ease of deployment. The primary drawback of quadrotors is that this are underactuated systems, which makes it challenging to perform maneuvers in tight or confined spaces. To address this challenge, a tilt-augmented quadrotor is presented in this paper. The initial exploration of this design concept is detailed in [1] and experimentally validated in [2]. In the work by [3], they achieved a successful tracking and landing of a tilt-augmented quadrotor on a moving vehicle, while maintaining desired roll and pitch angles at zero. In [4], they introduce a control law based on differential flatness for achieving aggressive maneuvers. However, this control approach doesn't decouple the position and orientation. On the other hand, in [5], a quasi time optimal control strategy for tilt-augmented quadrotor is used, ensuring stability even in the presence of constant disturbances during translational motion. In all these works, the control law stabilized the system, but they may not be robust to external disturbance and moment-of-inertia uncertainties. In [6], a robust linear controller is developed which effectively handles uncertainties in moment-of-inertia parameters but not external disturbances. In [7], a quaternion based robust controller is designed for tilt-quadrotor where the model is linearised about the zero angular velocity. The main drawback of using unit quaternions is their inherent ambiguity, as two different quaternions represent the same rotation. To achieve a globally unique representation, special orthogonal matrices ($SO(3)$) are employed to represent rigid body rotations [8].

Sathyanarayana Seshasayanan and Soumya Ranjan Sahoo are affiliated with the Department of Electrical Engineering at the Indian Institute of Technology Kanpur, Kanpur, India, {sathya,srsahoo}@iitk.ac.in

In a tilt-augmented quadrotor, the system's performance is influenced by both external disturbances and uncertainty in the moment-of-inertia. As a result, there is a requirement to design an adaptive STSMO, capable of estimating uncertain terms in a finite time, even when the uncertainty bounds remain unknown. Unlike conventional quadrotors, the tilt-augmented quadrotor has the ability to independently control the position and orientation. An adaptive STMSO and backstepping controllers based on $SO(3)$ are developed for the position and orientation control separately. This approach guarantees exponential convergence of the position and orientation of the tilt-augmented quadrotor to the desired trajectory even in presence of external disturbance and inertia uncertainties. Thus, the main advantages of the proposed approach is summarized as follows,

1. A finite time convergence of the estimation of the uncertain terms in the presence of an unknown uncertainty bound.

2. Exponential convergence of the position and orientation of the tilt-augmented quadrotor to the desired trajectory.

The paper's organization is as follows: Section II outlines the mathematical model for the tilt-augmented quadrotor. Section III introduces the adaptive STSMO in conjunction with the backstepping-based controller. Hardware results are showcased in Section IV, and a summary of the work can be found in Section V.

II. MATHEMATICAL MODELING

This section deals with the dynamic model of a tilt-augmented quadrotor. The readers are referred to [1], [3], [6] for detail mathematical model. The control torque $\mathbf{M}_b \in \mathbb{R}^3$ and the control force $\mathbf{F}_b \in \mathbb{R}^3$ are defined in body fixed frame. The thrust F_i and moments M_i generated by the i^{th} rotor are decomposed along the body-fixed frame using the tilt angles (α_i) as references. The control torque $\mathbf{M}_b \in \mathbb{R}^3$ and the force $\mathbf{F}_b \in \mathbb{R}^3$ with respect to tilt angles and rotor speeds are given in [6]. The kinematics governing the rotation of the tilt-augmented quadrotor can be expressed as follows:

$$\dot{\mathcal{R}} = \mathcal{R}\hat{\boldsymbol{\omega}}_b, \tag{1}$$

where $\mathcal{R} \in SO(3)$ representing the orientation of the body fixed frame with respect to the inertial frame. The rotation dynamic model of the tilt-augmented quadrotor in body fixed frame is described as follows [9],

$$\mathcal{J}\dot{\boldsymbol{\omega}}_b = \boldsymbol{\omega}_b \times \mathcal{J}\boldsymbol{\omega}_b + \mathbf{M}_b + \mathbf{T}_d. \tag{2}$$

where $\times$ is the cross product of two vectors, $\mathbf{T}_d \in \mathbb{R}^3$, $\boldsymbol{\omega}_b \in \mathbb{R}^3$, and $\mathcal{J} \in \mathbb{R}^{3\times3}$ represents disturbance torque, angular velocity, and the moment-of-inertia matrix in body fixed frame, respectively. The translation dynamics of the tilt-augmented quadrotor is given by,

$$m\ddot{\mathbf{p}} = \mathcal{R}\mathbf{F}_b + m[0,0,g]^\top + \mathbf{F}_d, \tag{3}$$

where $\mathbf{p} \in \mathbb{R}^3$ is the position vector with respect inertial frame, g is the acceleration due to gravity, m is the mass of the tilt-augmented quadrotor and $\mathbf{F}_d$ represents the disturbance force acting in inertial frame.

Based on dynamics and kinematics of the tilt-augmented quadrotor given in (1)-(3), uncertain terms are the force $\mathbf{F}_d$ and torque $\mathbf{T}_d$ disturbances and the moment-of-inertia $\mathcal{J}$. In the next section, we design an observer which attempts estimates the uncertain terms in finite time. Later with the help of this observer, we design a backstepping controller to track the desired trajectory.

III. STSM Observer and Control Design

The objective of this work is to make the tilt-augmented quadrotor to reach the desired position and orientation in presence of external disturbances and uncertain moment-of-inertia $\mathcal{J}$. The tilt-augmented quadrotor has the ability to independently control its force and torque in any direction [10]. This helps to design the controller for attitude and position separately. When the rotor tilts the moment-of-inertia changes. Thus it is necessary to design a robust controller for the tilt-augmented quadrotor dynamics. Based on dynamics given in (2), consider the nominal rotation dynamics given as,

$$\bar{\mathcal{J}}\dot{\bar{\boldsymbol{\omega}}}_b = \boldsymbol{\omega}_b \times \bar{\mathcal{J}}\boldsymbol{\omega}_b + \mathbf{M}_b + \bar{\mathbf{T}}_d, \tag{4}$$

where $\bar{\mathcal{J}}$ is nominal moment-of-inertia matrix, $\bar{\mathbf{T}}_d \in \mathbb{R}^3$ and $\bar{\boldsymbol{\omega}}_b \in \mathbb{R}^3$ are the estimation of the uncertain terms. Similarly given translation dynamics given in (3), the nominal linear velocity dynamics of the tilt-augmented quadrotor is given by,

$$m\dot{\bar{\mathbf{v}}} = \mathcal{R}\mathbf{F}_b + m[0,0,g]^\top + \bar{\mathbf{F}}_d, \tag{5}$$

Next we design a observer such that $\bar{\boldsymbol{\omega}}_b$ converges to $\boldsymbol{\omega}_b$ and $\bar{\mathbf{v}}$ converges to $\dot{\mathbf{p}}$ in finite time and design the backstepping based controller to track the desired trajectory.

A. STSMO for Rotational Dynamics

The primary objective is for $\bar{\boldsymbol{\omega}}_b$ to converge to $\boldsymbol{\omega}_b$ within a finite time. To achieve this, a conventional super-twisting sliding mode based observer is developed. Consider sliding surface $\boldsymbol{\sigma} := [\sigma_1, \sigma_2, \sigma_3] \in \mathbb{R}^3$, defined as:

$$\boldsymbol{\sigma} = \bar{\mathcal{J}}\boldsymbol{\omega}_b - \bar{\mathcal{J}}\bar{\boldsymbol{\omega}}_b \tag{6}$$

Using (2), and (6), the time derivative of the $\boldsymbol{\sigma}$ is

$$\dot{\boldsymbol{\sigma}} = \mathbf{M}_d - \bar{\mathbf{T}}_d \tag{7}$$

where $\mathbf{M}_d = \mathbf{T}_d + (\bar{\mathcal{J}} - \mathcal{J})\dot{\boldsymbol{\omega}}_b - \boldsymbol{\omega}_b \times (\bar{\mathcal{J}} - \mathcal{J})\boldsymbol{\omega}_b$ be the cumulative uncertain terms. Based on STSMC structure [11], $\bar{\mathbf{T}}_d$ in (4) can be designed as,

$$\begin{aligned} \bar{\mathbf{T}}_d &= k_1\mathbf{M}_v + \mathbf{T}_w \\ \dot{\mathbf{T}}_w &= k_2 \text{sign}(\boldsymbol{\sigma}) \end{aligned} \tag{8}$$

where $\mathbf{M}_v = [\sqrt{|\sigma_1|}\text{sign}(\sigma_1), \sqrt{|\sigma_2|}\text{sign}(\sigma_2), \sqrt{|\sigma_3|}\text{sign}(\sigma_3)]$, and $k_1 = \text{diag}([k_{1,1}, k_{1,2}, k_{1,3}])$, $k_2 = \text{diag}([k_{2,1}, k_{2,2}, k_{2,3}])$ are adaptive gain matrices. The adaptive law for the gain matrices is

$$\dot{k}_{(1,i)} = \begin{cases} \omega\sqrt{\dfrac{\gamma}{2}}, & \text{if } \sigma_i \neq 0 \\ 0, & \text{else} \end{cases}, \ \forall i = [1,2,3]. \tag{9}$$

where $k_{(2,i)} = 0.5\epsilon k_{(1,i)}$, $k_{1,i}(0) > 0, \forall i = [1,2,3]$ and ω, γ, ϵ are positive constant.

Lemma 1: Suppose the derivative of $\mathbf{M_d}$ is bounded, that is, $||\dot{\mathbf{M}}_d||_\infty \leq D \in \mathbb{R}^+$. For the system (7) and $\bar{\mathbf{T}}_d$ given in (8), with the adaptive gains k_1 and k_2 given in (9), then both $\boldsymbol{\sigma}$ and $\dot{\boldsymbol{\sigma}}$ converge to $[0,0,0]^\top$ in finite time T.
The detailed proof of the Lemma 1 is discussed in proposition 2 of [12].

From Lemma 1, both $\boldsymbol{\sigma}$ and $\dot{\boldsymbol{\sigma}}$ converge to $[0,0,0]^\top$ in finite time T. Thus from (7), $\bar{\mathbf{T}}_d(t) = \mathbf{M}_d(t)$, $\forall t > T$. From the proof of Lemma 1 $\boldsymbol{\sigma}$ is a decreasing function with respect to time [12]. Thus, for $\forall t \leq T$, the magnitude of $||\bar{\mathbf{T}}_d - \mathbf{M}_d||_2$ remains bounded, that is, $||\bar{\mathbf{T}}_d - \mathbf{M}_d||_2 \leq \epsilon_a \in \Re^+$.

B. Backstepping Controller for Rotation Dynamics

The goal here is to design the control torque $\mathbf{M}_b$ in a way that aligns the body-fixed frame with the desired frame. Let the desired orientation with respect to inertial frame be denoted as $\mathcal{R}_d$. The orientation of body fixed frame with respect to the inertial frame is defined as,

$$\mathcal{R}_e = \mathcal{R}_d^\top \mathcal{R} \tag{10}$$

The objective here is to design the controller such that $\mathcal{R} = \mathcal{R}_d$, that is $\mathcal{R}_e = I_3$. Thus the candidate error function $\Psi : SO(3) \to \mathbb{R}$ [13] be defined as,

$$\Psi = \frac{1}{2}\,\text{tr}\{K(I_3 - \mathcal{R}_e)\} \tag{11}$$

where K is positive diagonal matrix with distinct eigen values. Using rotation kinematics, the desired angular velocity $\boldsymbol{\omega}_d$ is calculated as,

$$\widehat{\boldsymbol{\omega}}_d = \mathcal{R}_d^\top \dot{\mathcal{R}}_d. \tag{12}$$

The $\boldsymbol{\omega}_d$ is in desired frame, and $\boldsymbol{\omega}$ is in body fixed frame. Since there are in different frames of reference, the angular velocity error is defined as,

$$\boldsymbol{\omega}_e = \boldsymbol{\omega}_b - \mathcal{R}_e^\top \boldsymbol{\omega}_d, \tag{13}$$

The time derivative of Ψ is given by [14],

$$\dot{\Psi} = \mathbf{e}_R^\top \boldsymbol{\omega}_e, \tag{14}$$

where $\mathbf{e}_R = \frac{1}{2}(K\mathcal{R}_e - \mathcal{R}_e^\top K)^\vee$. The Ψ is both upper and lower bounded by,

$$b_1||\mathbf{e}_R||_2^2 \leq \Psi \leq b_2||\mathbf{e}_R||_2^2 \tag{15}$$

where b_1 and b_2 are positive constant. The proof of (15) and expression of b_1 and b_2 are given in [14]. Consider the Lyapunov candidate as (11), using (14) and (13), the control input for $\boldsymbol{\omega}_b$ is

$$\boldsymbol{\omega}_u = -K_r\mathbf{e}_r + \mathcal{R}_e^\top \boldsymbol{\omega}_d. \tag{16}$$

where K_r is the positive definite matrix. The time derivative of $\boldsymbol{\omega}_u$ is

$$\dot{\boldsymbol{\omega}}_u = -K_r(K\mathcal{R}_e\widehat{\boldsymbol{\omega}}_e + \widehat{\boldsymbol{\omega}}_e\mathcal{R}_e^\top K)^\vee + \mathcal{R}_e^\top\dot{\boldsymbol{\omega}}_d - \widehat{\boldsymbol{\omega}}_e\mathcal{R}_e^\top\boldsymbol{\omega}_d. \tag{17}$$

From (14), if $\boldsymbol{\omega}_u = \boldsymbol{\omega}_b$ then $\dot{\Psi} = -\mathbf{e}_r^\top K_r\mathbf{e}_r$. Thus the angular velocity error is defined as,

$$\mathbf{e}_\omega = \boldsymbol{\omega}_u - \boldsymbol{\omega}_b. \tag{18}$$

The augmented Lyapunov function is take as,

$$V_3 = \Psi + \frac{1}{2}\mathbf{e}_\omega^\top \bar{J}\mathbf{e}_\omega \tag{19}$$

Using (2) and (16), the time derivative V_3 is

$$\dot{V}_3 = -\mathbf{e}_r^\top K_r\mathbf{e}_r + \mathbf{e}_\omega^\top(\bar{J}\dot{\boldsymbol{\omega}}_u - \mathbf{M}_b - \mathbf{M}_d - \boldsymbol{\omega}_b \times \bar{J}\boldsymbol{\omega}_b - \mathbf{e}_r) \tag{20}$$

Using (20), the control torque $\mathbf{M}_b$ is

$$\mathbf{M}_b = -\mathbf{e}_r - \boldsymbol{\omega}_b \times \bar{J}\boldsymbol{\omega}_b - \bar{\mathbf{T}}_d + K_w\mathbf{e}_w + \bar{J}\dot{\boldsymbol{\omega}}_u. \tag{21}$$

Using (21), the (20) reduces to,

$$\dot{V}_3 = -\mathbf{e}_r^\top K_r\mathbf{e}_r - \mathbf{e}_\omega^\top K_w\mathbf{e}_\omega - \mathbf{e}_\omega^\top(\bar{\mathbf{T}}_d - \mathbf{M}_d) \tag{22}$$

From Section III-A, $\forall t \leq T$, $||\bar{\mathbf{T}}_d - \mathbf{M}_d||_2 \leq \epsilon_a$, and $\forall t > T$ $\bar{\mathbf{T}}_d = \mathbf{M}_d$.

Theorem 1: For the system (2), with control law given in (21) and observer given in (8), for time $t < T$ the error $\mathbf{e}_\omega$ remains bounded by,

$$||\mathbf{e}_\omega||_2 \leq \max\left\{||\mathbf{e}_\omega(0)||_2, \frac{\epsilon_a}{\lambda_{min}(K_w)}\right\} \tag{23}$$

and for time $t > T$, both $\mathbf{e}_\omega$ and $\mathbf{e}_r$ reaches $[0,0,0]^\top$ exponentially.

Proof: When time $t < T$, consider the augmented Lyapunov function given in (19) and its derivative given in (22). The $\dot{V}_3$ is lower bounded by,

$$\dot{V}_3 \leq -\lambda_{min}(K_r)||\mathbf{e}_r||_2^2 - \lambda_{min}(K_w)||\mathbf{e}_\omega||_2^2 + ||\mathbf{e}_\omega||_2\epsilon_a \tag{24}$$

The $\dot{V}_3$ is negative for the region when,

$$||\mathbf{e}_\omega||_2 \geq \frac{\epsilon_a}{\lambda_{min}(K_w)}. \tag{25}$$

Since $\dot{V}_3$ is negative outside the region $||\mathbf{e}_\omega||_2 \leq \frac{\epsilon_a}{\lambda_{min}(K_w)}$, thus $\mathbf{e}_\omega$ remains bounded and the bound is given in (23) for time $t < T$. When time $t \geq T$, from Lemma 1, $\mathbf{M}_d = \bar{\mathbf{T}}_d$. Using this, we have (22) as,

$$\begin{aligned}\dot{V}_3 &\leq -\min(\lambda_{min}(K_w), \lambda_{min}(K_r))(||\mathbf{e}_\omega||_2^2 + ||\mathbf{e}_r||_2^2) \\ \dot{V}_3 &\leq -2\min\left(\lambda_{min}(K_w), \frac{\lambda_{min}(K_r)}{b_2}\right)V_3.\end{aligned} \tag{26}$$

Thus from the expression (26), the controller given in (21) and (8), after time T_p, both $\mathbf{e}_r$ and $\mathbf{e}_\omega$ converge to $[0,0,0]^T$ exponentially. ■

C. STSMO for Translation Dynamics

The objective here is to design the observer such that $\bar{\mathbf{v}}$ converges to $\dot{\mathbf{p}}$ in finite time. Let the sliding surface $\boldsymbol{\upsilon} := [\upsilon_1, \upsilon_2, \upsilon_3] \in \mathbb{R}^3$ be defined as,

$$\boldsymbol{\upsilon} = m\dot{\mathbf{p}} - m\bar{\mathbf{v}}. \tag{27}$$

Using (3), (27), the time derivative of the $\boldsymbol{\upsilon}$ is

$$\dot{\boldsymbol{\upsilon}} = \bar{\mathbf{F}}_d - \mathbf{F}_d. \tag{28}$$

Based on super twisting sliding mode controller (STSMC) [11], $\bar{\mathbf{F}}_d$ in (28) can be designed as,

$$\begin{cases}\bar{\mathbf{F}}_d = k_3\mathbf{f}_v + \mathbf{f}_w \\ \dot{\mathbf{f}}_w = k_4\text{sign}(\boldsymbol{\upsilon})\end{cases} \tag{29}$$

where $\bar{\mathbf{f}}_v = [\sqrt{|\upsilon_1|}\text{sign}(\upsilon_1), \sqrt{|\upsilon_2|}\text{sign}(\upsilon_2), \sqrt{|\upsilon_3|}\text{sign}(\upsilon_3)]^\top$, and $k_3 = \text{diag}([k_{3,1}, k_{3,2}, k_{3,3}])$, $k_4 = \text{diag}([k_{4,1}, k_{4,2}, k_{4,3}])$ are adaptive gain matrices. The adaptive law for the gain matrices is

$$\dot{k}_{(3,i)} = \begin{cases}\omega\sqrt{\frac{\gamma}{2}}, & \text{if } |\upsilon_i| \neq 0 \\ 0, & \text{else}\end{cases}, \ \forall i = [1,2,3]. \tag{30}$$

where $k_{(4,i)} = 0.5\epsilon k_{(3,i)}$, $k_{3,i}(0) > 0, \forall i = [1,2,3]$ and ω, γ, ϵ are positive constant.

Lemma 2: Suppose the derivative of $\mathbf{F_d}$ is bounded, that is, $||\dot{\mathbf{F}}_d||_\infty \leq D_1 \in \mathbb{R}^+$. For the system (28) and $\bar{\mathbf{F}}_d$ given in (29), with the adaptive gains k_3 and k_4 given in (30), then $\boldsymbol{\upsilon}$ and $\dot{\boldsymbol{\upsilon}}$ converge to $[0,0,0]^\top$ in finite time T_p.

The detailed proof of the Lemma 2 is discussed in proposition 2 of [12]. From Lemma 2, both $\boldsymbol{\upsilon}$ and $\dot{\boldsymbol{\upsilon}}$ converge to $[0,0,0]^\top$ in finite time T_1. This implies that from (28), $\bar{\mathbf{F}}_d$ converges to $\mathbf{F}_d$ in finite time T_p. From the proof of Lemma 2 $\boldsymbol{\upsilon}$ is a decreasing function with respect to time [12]. Thus, for the time $0 \leq t \leq T_p$, difference between $\bar{\mathbf{F}}_d$ and $\mathbf{F}_d$ remains bound which is given by $||\bar{\mathbf{F}}_d - \mathbf{F}_d|| \leq \epsilon_p \in \Re^+$.

D. BackStepping Controller for Translation Dynamics

Let $\mathbf{F}_w = \mathcal{R}\mathbf{F}_b + m[0,0,g]^\top$ be the control force in the inertial frame. From (3), linear dynamics reduces to,

$$m\ddot{\mathbf{p}} = \mathbf{F}_w + \mathbf{F}_d. \tag{31}$$

From Section III-C, we know that $\bar{\mathbf{F}}_d$ converges to $\mathbf{F}_d$ in finite time, thus we design the control force as $\mathbf{F}_w = \mathbf{F}_c - \bar{\mathbf{F}}_d$. The objective here is to design $\mathbf{F}_c$ such that $\mathbf{p}$ tracks

the desired position $\mathbf{p}_d$. For this a backsteeping control law is developed. The translation error $\mathbf{e}_p$ be defined as,

$$\mathbf{e}_p = \mathbf{p}_d - \mathbf{p}. \tag{32}$$

Let a positive definite Lyapunov function in terms of $\mathbf{e}_p$ is

$$V_1 = \frac{1}{2}\mathbf{e}_p^\top \mathbf{e}_p \tag{33}$$

The time derivative of $\mathbf{e}$ is $\dot{\mathbf{e}}_p = \dot{\mathbf{p}}_d - \dot{\mathbf{p}}$. Assuming $\dot{\mathbf{p}}$ to be the control input for the $\dot{\mathbf{e}}_p$, the control law for $\dot{\mathbf{p}}$ is

$$\dot{\mathbf{p}}_u = \dot{\mathbf{p}}_d + K_p \mathbf{e}_p. \tag{34}$$

where K_p is a positive definite matrix. If $\dot{\mathbf{p}}_u = \dot{\mathbf{p}}$ then $\dot{V}_1$ in (33) turns out to be $\dot{V}_1 = -\mathbf{e}_p^\top K_p \mathbf{e}_p < 0$. Thus, the error between $\dot{\mathbf{p}}_u$ and $\dot{\mathbf{p}}$ be defined as,

$$\mathbf{e}_v = \dot{\mathbf{p}}_d + K_p \mathbf{e}_p - \dot{\mathbf{p}} \tag{35}$$

Let the augmented Lyapunov function be defined as,

$$V_2 = \frac{1}{2}\mathbf{e}_p^\top \mathbf{e}_p + \frac{1}{2}\mathbf{e}_v^\top \mathbf{e}_v \tag{36}$$

Using (34) (35), the time derivative of V_2 is given by,

$$\dot{V}_2 = \mathbf{e}_v^\top (\mathbf{e}_p + \ddot{\mathbf{p}}_d + K_p \dot{\mathbf{e}}_p - \ddot{\mathbf{p}}) - \mathbf{e}_p^\top K_p \mathbf{e}_p \tag{37}$$

Using (37), the control law is given by,

$$\mathbf{F}_w = m(\mathbf{e}_p + \ddot{\mathbf{p}}_d + K_p \dot{\mathbf{e}}_p + K_v \mathbf{e}_v) - \bar{\mathbf{F}}_d, \tag{38}$$

where K_v is a positive definite matrix. From (38), the $\mathbf{F}_b$ is

$$\mathbf{F}_b = \mathcal{R}^\top (\mathbf{F}_w - m[0, 0, g]^\top). \tag{39}$$

Substituting (38) in (37) we get,

$$\dot{V}_2 = -\mathbf{e}_v^\top K_v \mathbf{e}_v - \mathbf{e}_p^\top K_p \mathbf{e}_p + \mathbf{e}_v^\top (\bar{\mathbf{F}}_d - \mathbf{F}_d). \tag{40}$$

From Section III-C, $\bar{\mathbf{F}}_d$ converges to $\mathbf{F}_d$ in finite time T_p.

Theorem 2: For the system (3), with controller law given in (38) and observer given in (29), for time $t < T_p$,

$$||\mathbf{e}_v||_2 \leq \max\left\{||\mathbf{e}_v(0)||_2, \frac{\epsilon_p}{\lambda_{min}(K_v)}\right\} \tag{41}$$

and for time $t \geq T_p$, $\mathbf{e}_p$ and $\mathbf{e}_v$ exponentially converges to $[0, 0, 0]^\top$.

Using proof given in Theorem 1, a similar steps is followed to prove Theorem 2.

Remark 1: In practical implementation, the controllers are discretized using Euler approximation, and the presence of noise in the sensor data can introduce residual errors in the feedback signal. As a result, the sliding surfaces $\boldsymbol{\upsilon}$ and $\boldsymbol{\sigma}$ do not converge to zero in finite time. This lack of convergence causes the adaptive gains given in (30) and (9) to remain unbounded. To address this issue and bound the gains, the adaptive law is modified as proposed in [12],

$$\dot{k}_{(3,i)} = \begin{cases} \omega\sqrt{\frac{\gamma}{2}}\text{sign}(|\upsilon_i| - \mu_1), & \text{if } k_{3,i} > k_m \\ \eta, & \text{else} \end{cases}, \tag{42}$$

$$\dot{k}_{(1,i)} = \begin{cases} \omega\sqrt{\frac{\gamma}{2}}\text{sign}(|\sigma_i| - \mu_2), & \text{if } k_{1,i} > k_m \\ \eta, & \text{else} \end{cases}, \tag{43}$$

where η, k_m is positive constant, μ_1, μ_2 are small positive constant, $k_{3,i}(0) > k_m$ and $k_{1,i}(0) > k_m$.

The map from control torques (21) and forces (39) to corresponding rotor speeds and tilt angles is in [10].

IV. Results

A. Control Parameters

The selection of gain matrices for the position backstepping controller (K_p, K_v) and the orientation backstepping controller (K_r, K_w) must ensure that the controller bandwidth requirements are met. As the rate of convergence increases, the controller's bandwidth also increases. Thus, the maximum convergence rate is limited by the bandwidth of the controller. From Theorem 2 and Theorem 1, which describe the exponential convergence of errors to zero, the maximum exponential rate of V_2 for time $t > T_p$ can be calculated using (36) and (40) as:

$$\dot{V}_2 \geq -2\delta_p V_2 \tag{44}$$

where $\delta_p = \max\{\lambda_{max}(K_p), \lambda_{max}(K_v)\}$. From (36), since $\mathbf{e}_p$ and $\mathbf{e}_v$ are quadratic in V_2, the maximum convergence rate of $\mathbf{e}_p$ and $\mathbf{e}_v$ is given by δ_p.

Similarly, for time $t > T$, the maximum exponential rate of V_3 using (19) and (22) is given by,

$$\dot{V}_3 \geq -2\delta_a V_3 \tag{45}$$

where $\delta_a = \dfrac{\max\{\lambda_{max}(K_r), \lambda_{max}(K_w)\}}{\min\{b_1, \lambda_{min}(\bar{\mathcal{J}})\}}$. Thus the maximum exponential rate of $\mathbf{e}_r$ and $\mathbf{e}_w$ is δ_a. For a linear system, the exponential rate of convergence is equivalent to the system's bandwidth. Consequently, the choice of gain matrices is based on the required bandwidth of the controller. It's worth noting that increasing the adaptive gain parameters $(\gamma, \epsilon, \omega)$ results in more chattering in the observer. Therefore, the adaptive gain parameters are carefully chosen to minimize chattering in disturbance estimation.

The controller gains used in the this paper are given in Table. I.

TABLE I: Controller gain values

Parameters	Values	Parameters	Values
K_p	diag([1, 1, 1])	ω	1
K_v	diag([2, 2, 2])	ϵ	0.1
K	diag([1, 1.2, 1.3])	μ_1	0.01
K_r	diag([3, 3, 3])	μ_2	0.001
K_w	0.2diag([1, 1, 1])	η	0.1
γ	2	k_m	0.05

B. Hardware Results

1) Hardware Description: Figure 1 shows the tilt quadcopter developed in-house that has been used for the experiments. The main frame of the tilt quadrotor is made up of carbon fiber tubes and plates. Each arm is equipped with a dual-shaft servo motor positioned at its extremities. We used

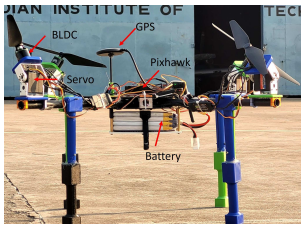

Fig. 1: Tilt-augmented quadrotor developed in-house.

Pixhawk 2.4.8 [15] running PX4 firmware version 1.10.2. Communication between the vehicle and the ground station is facilitated by a 433 MHz telemetry module. Additionally, a global positioning system (GPS) receiver provides global position feedback. In this experiment, a waypoints in position and step command for orientation is given as reference. The waypoints are selected to form a rectangle, with the four points labeled as A([0,0,-5]), B([0,-20,-5]), C([9.5,-20,-5]), D([10.5,0,-5]). When the vehicles reaches a safe height from the ground a switch from the radio transmitter is triggered to set the desired attitude. The desired attitude for the roll (ϕ), pitch (θ) and yaw (ψ) is set as $[10^\circ, 10^\circ, 0^\circ]^\top$. For ease of visualization, Euler angles are employed to depict the results. For the conversion of rotation matrices to Euler angles and vice versa, readers are directed to [16].

2) Existing Work: Here, the performance of the existing quasi-time optimal control (QTOC) designed in [5] is tested on our tilt quadrotor. Given the waypoint, the position tracking for QTOC is shown in Fig. 2. From the figures, it is observed that the vehicle takes 8 seconds to reach point A from the ground with tolerance band of ± 0.5 m. From waypoint A, the vehicle takes 10 seconds to reach waypoint B with a tolerance band of ± 0.5 m. From waypoint B, at the start, the vehicle undershoots to 2 m and reaches waypoint C in 10 seconds; this may be due to external disturbance. From point C, the vehicle moves to waypoint C in 10 seconds and then to waypoint D in 5 seconds.

In Fig. 3, the attitude tracking performance of the existing QTO controller designed in [5] is illustrated. As observed in Fig. 3, the vehicle undergoes oscillations of magnitude $\pm 2^\circ$ and $\pm 4^\circ$ from the setpoint for roll and pitch, respectively. The settling time with a tolerance band of $\pm 2^\circ$ is 1 second for roll, and pitch.

3) Proposed Controller: Here, the performance of the proposed controller discussed in Section III with the control parameters given in Table I is evaluated. Given the waypoint, the position tracking of the proposed controller is shown in Fig. 4. From the figures, it is observed that the vehicle takes 8 seconds to reach point A with a tolerance band of ± 0.5 m. The vehicle takes 10, 5, and 10 seconds to move from A to B, B to C, and C to D, respectively.

In Fig. 3, the attitude tracking performance of the proposed controller designed in Section III-A is illustrated. As observed in Fig. 3, the vehicle settles within $\pm 2^\circ$ tolerance band for roll, and pitch. The vehicle settles within $\pm 2^\circ$, $\pm 2^\circ$ and $\pm 2.2^\circ$ for roll, pitch and yaw, respectively.

From the position tracking of the proposed controller and the existing controller presented in Figs. 2 and 4, it is observed that the existing controller overshoots due to the presence of external disturbance, which is not the case for the proposed controller. Similarly, for the attitude tracking presented in Figs. 3 and 5 of the proposed controller and existing controller, it is observed that the existing controller oscillates $\pm 4^\circ$ in pitch, whereas the proposed controller remains within $\pm 2^\circ$. Thus, the proposed backstepping controller with adaptive STSMO outperforms the existing QTOC [5] in terms of overshoot and steady state performances. The video of this experiment can be seen in https://www.youtube.com/watch?v=brTd5UYvciM

V. Conclusion

This paper discuss the development of a robust controller for the tilt-augmented quadrotor. In a tilt-augmented quadrotor, the system's performance is affected by external disturbances and uncertainties in moment-of-inertia. Unlike conventional quadrotors, the tilt-augmented quadrotor has ability to independently control the position and orientation. Thus, in this work, an adaptive super twisting sliding mode observer is designed for position and orientation separately to estimate the uncertainty terms in finite time. The backstepping stepping controller based on $SO(3)$ is designed assuring exponential convergence towards the desired trajectory. The experiments are carried out in outdoors to validate the performance of the controller. The results indicate that the proposed combination of the adaptive super-twisting sliding mode observer (STSMO) with a backstepping controller exhibits superior tracking performance in comparison to the existing controller designed for the tilt-augmented quadrotor.

References

[1] M. Ryll, H. H. Bülthoff, and P. R. Giordano, "Modeling and control of a quadrotor uav with tilting propellers," in *2012 IEEE International Conference on Robotics and Automation*, 2012, pp. 4606–4613.

[2] M. Ryll, H. H. Bülthoff, and P. R. Giordano, "A novel overactuated quadrotor unmanned aerial vehicle: Modeling, control, and experimental validation," *IEEE Transactions on Control Systems Technology*, vol. 23, no. 2, pp. 540–556, 2015.

[3] M. Bhargavapuri, A. K. Shastry, H. Sinha, S. R. Sahoo, and M. Kothari, "Vision-based autonomous tracking and landing of a fully-actuated rotorcraft," *Control Engineering Practice*, vol. 89, pp. 113–129, 2019.

[4] R. Kumar, A. Nemati, M. Kumar, R. Sharma, K. Cohen, and F. Cazaurang, "Tilting-rotor quadcopter for aggressive flight maneuvers using differential flatness based flight controller," in *Dynamic Systems and Control Conference*, vol. 3, 2017.

[5] D. Invernizzi, M. Giurato, P. Gattazzo, and M. Lovera, "Full pose tracking for a tilt-arm quadrotor uav," in *IEEE Conference on Control Technology and Applications (CCTA)*, 2018, pp. 159–164.

[6] S. Seshasayanan and S. R. Sahoo, "Robust linear controller design for tilt quadrotor based on euler angles," in *2022 Eighth Indian Control Conference (ICC)*, 2022, pp. 218–223.

[7] S. Seshasayanan, S. De, and S. R. Sahoo, "Robust attitude control with fixed exponential rate of convergence and consideration of motor dynamics for tilt quadrotor using quaternions," *IEEE Transactions on Automation Science and Engineering*, pp. 1–15, 2024.

[8] S. Berkane, A. Abdessameud, and A. Tayebi, "Hybrid output feedback for attitude tracking on $\mathbb{SO}(3)$," *IEEE Transactions on Automatic Control*, vol. 63, no. 11, pp. 3956–3963, 2018.

[9] M. De Lellis Costa de Oliveira, "Modeling, identification and control of a quadrotor aircraft," Ph.D. dissertation, Czech Technical University in Prague, 06 2011.

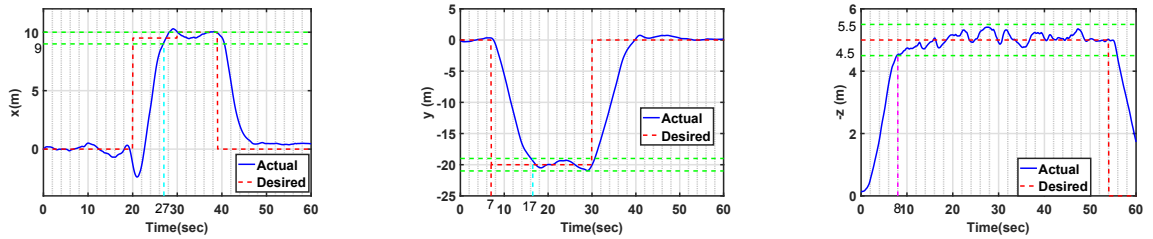

(a) Inertial frame $x-$axis (b) Inertial frame $y-$axis (c) Inertial frame $z-$axis

Fig. 2: Position Tracking of the tilt-augmented quadrotor for the existing QTO controller

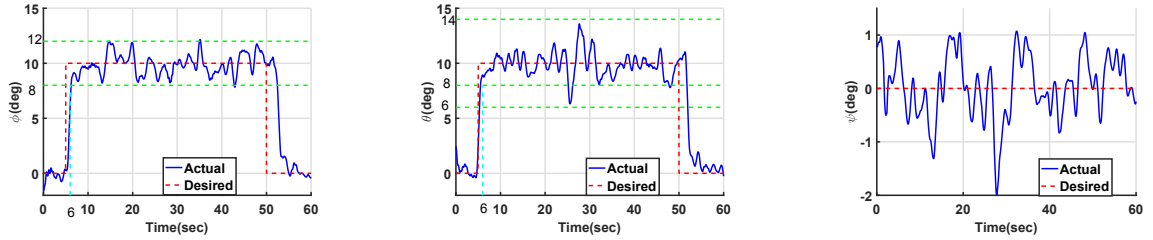

(a) Roll (b) Pitch (c) Yaw

Fig. 3: Attitude tracking of the tilt-augmented quadrotor for the existing QTO controller

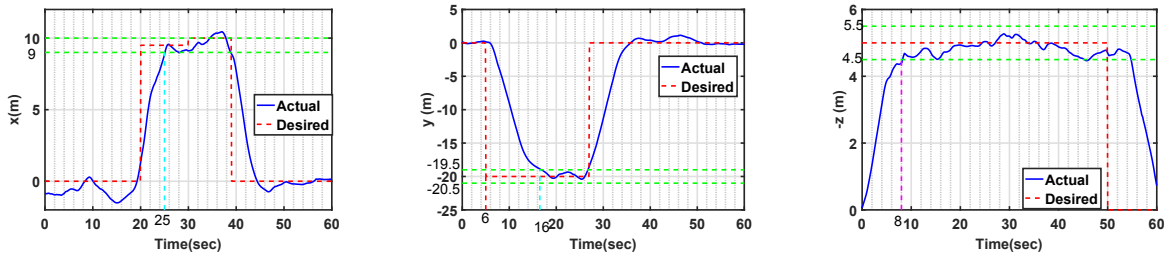

(a) Inertial frame $x-$axis (b) Inertial frame $y-$axis (c) Inertial frame $z-$axis

Fig. 4: Position Tracking of the tilt-augmented quadrotor for the proposed controller

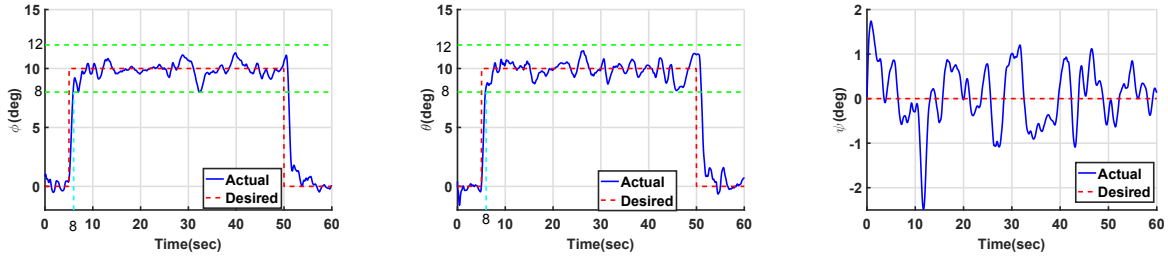

(a) Roll (b) Pitch (c) Yaw

Fig. 5: Attitude tracking of the tilt-augmented quadrotor for the proposed controller

[10] D. Invernizzi, M. Giurato, P. Gattazzo, and M. Lovera, "Comparison of control methods for trajectory tracking in fully actuated unmanned aerial vehicles," *IEEE Transactions on Control Systems Technology*, vol. 29, no. 3, pp. 1147–1160, 2021.

[11] D. Ao, W. Huang, P. K. Wong, and J. Li, "Robust backstepping super-twisting sliding mode control for autonomous vehicle path following," *IEEE Access*, vol. 9, pp. 123 165–123 177, 2021.

[12] Y. Shtessel, M. Taleb, and F. Plestan, "A novel adaptive-gain supertwisting sliding mode controller: Methodology and application," *Automatica*, vol. 48, no. 5, pp. 759–769, 2012. [Online]. Available: https://www.sciencedirect.com/science/article/pii/S0005109812000751

[13] T. Lee, "Robust global exponential attitude tracking controls on so(3)," in *2013 American Control Conference*, 2013, pp. 2103–2108.

[14] T. Fernando, J. Chandiramani, T. Lee, and H. Gutierrez, "Robust adaptive geometric tracking controls on so(3) with an application to the attitude dynamics of a quadrotor uav," in *2011 50th IEEE Conference on Decision and Control and European Control Conference*, 2011, pp. 7380–7385.

[15] L. Meier, D. Honegger, and M. Pollefeys, "Px4: A node-based multithreaded open source robotics framework for deeply embedded platforms," in *2015 IEEE International Conference on Robotics and Automation (ICRA)*, 2015, pp. 6235–6240.

[16] D. M. Henderson, "Euler angles, quaternions, and transformation matrices for space shuttle analysis," *NTRS*, p. 12–24, 1977. [Online]. Available: https://ntrs.nasa.gov/citations/19770019231